THE JOURNAL OF BIOLOGICAL CHEMISTRY VOL. 284, NO. 31, pp. 20830–20839, July 31, 2009

Inhibition of Tau Polymerization with a Cyanine Dye in Two Distinct Model Systems*

Received for publication, May 1, 2009, and in revised form, May 22, 2009 Published, JBC Papers in Press, May 28, 2009, DOI 10.1074/jbc.M109.016089

Erin E. Congdon[‡], Yvette H. Figueroa[‡], Lili Wang[‡], Galina Toneva[‡], Edward Chang[§], Jeff Kuret[¶], Christopher Conrad[‡], and Karen E. Duff[‡1]

From the [‡]Department of Pathology, Taub Institute, Columbia University and Department of Integrative Neuroscience, New York State Psychiatric Institute, New York, New York 10032 and the [§]Integrated Biomedical Science Program and [¶]Department of Cellular and Molecular Biology, Ohio State University, Columbus, Ohio 43210

In a host of neurodegenerative diseases Tau, a microtubule-associated protein, aggregates into insoluble lesions within neurons. Previous studies have utilized cyanine dyes as Tau aggregation inhibitors *in vitro*. Herein we utilize cyanine dye 3,3′-diethyl-9-methyl-thiacarbocyanine iodide (C11) to modulate Tau polymerization in two model systems, an organotypic slice culture model derived from Tau transgenic mice and a split green fluorescent protein complementation assay in Tau-expressing cells. In slice cultures, submicromolar concentrations (0.001 μM) of C11 produced a significant reduction of aggregated Tau and a corresponding increase in unpolymerized Tau. In contrast, treatment with a 1 μM dose promoted aggregation of Tau. These results were recapitulated in the complementation assay where administration of 1 μM C11 produced a significant increase in polymerized Tau relative to control, whereas treatment of cells with 0.01 μM C11 resulted in a marked reduction of aggregated Tau. In the organotypic slice cultures, modulation of Tau aggregation was independent of changes in phosphorylation at disease and microtubule binding relevant epitopes for both dosing regimes. Furthermore, treatment with 0.001 μM C11 resulted in a decrease in both total filament mass and number. There was no evidence of apoptosis or loss of synaptic integrity at either dose, however, whereas submicromolar concentrations of C11 did not interfere with microtubule binding, higher doses resulted in a decrease in the levels of microtubule-bound Tau. Overall, a cyanine dye can dissociate aggregated Tau in an *ex vivo* model of tauopathy with little toxicity and exploration of the use of these type of dyes as therapeutic agents is warranted.

Abnormal accumulation of aggregated proteins is a common feature of many neurodegenerative disorders including Parkinson, Huntington, and Alzheimer diseases. The defining lesions in Alzheimer disease include the extracellular plaques composed of amyloid β and intracellular polymers of the microtubule-associated protein Tau. Under normal conditions, as much as 90% of the Tau expressed in neurons is bound to microtubules providing stability for the cytoskeleton. In addition, Tau may also play a role in the microtubule interactions of both Golgi membranes and dynein (1, 2).

Intracellular Tau aggregates are a defining feature in a host of neurodegenerative disorders including Alzheimer disease, corticobasal degeneration, and frontotemporal dementia. Development of neurofibrillary pathology in Alzheimer disease follows a highly stereotyped pattern (3, 4) and the appearance of tangles correlates with both neuronal loss and severity of cognitive symptoms (5–7). Evidence suggests that Tau polymerization may also be directly linked to degeneration. Mutations in the Tau gene are sufficient to cause familial cases of frontotemporal dementia and the disease causing mutations have been shown to alter the propensity for secondary structure and to promote Tau aggregation *in vitro* (8–10). Transgenic animals expressing aggregation-prone mutant Tau develop synaptic dysfunction (11). In contrast, animals expressing Tau containing an aggregation-inhibiting mutation displayed no changes in synapse number despite similar levels of hyperphosphorylation (11). Neurons containing Tau polymers have also been shown to have both accumulation of pro-apoptotic caspases as well as signaling deficits (12, 13). Impaired neurotransmission and morphological changes were observed in lesion-bearing neurons in a *Caenorhabditis elegans* model of tauopathy (14). Additionally, abnormal Tau aggregates have also been found to affect both gene transcription and proteasome activity (15, 16). In cell culture models higher levels of Tau polymerization was correlated with increased cell death (17, 18). Conversely, treatment with Tau aggregation inhibitors reduced levels of cell loss (18, 19). These findings indicate that development of Tau aggregation inhibitors is a potential avenue for the creation of disease modifying therapies.

A number of polymerization inhibitors have been studied including Congo red derivatives, anthraquinones (Pickhardt *et al.* (20), disputed in Crowe *et al.* (21)), 2,3-di(furan-2-yl)-quinoxalines (21), phenylthiazolylhydrazide (22, 23), polyphenols and porphyrins (24), and cyanine dyes (25–27). Cyanine dyes were identified in a small molecule screen as Tau fibrillization antagonists. Of these, 3-(2-hydroxyethyl)-2-[2-[[3-(2-hydroxyethyl)-5-methoxy-2-benzthiazolylidene]methyl]-1-butenyl]-5-methoxybenzothiazolium (N744)[2] has been well characterized

* This work was supported, in whole or in part, by National Institutes of Health Grants NS047447 (to K. D.) and AG14452 (to J. K.) from the NINDS. This work was also supported by the Alzheimer Drug Discovery Foundation/Institute for the Study of Aging, a Rosalinde and Arthur Gilbert Foundation/American Federation for Aging Research New Investigator Award in Alzheimer Disease, and the American Health Assistance Foundation.

[1] To whom correspondence should be addressed: P&S 12th Floor, Rm. 12-461, Columbia University Medical Center, New York, NY 10032. Tel.: 212-305-8970; Fax: 212-342-0119; E-mail: ked2115@columbia.edu.

[2] The abbreviations used are: N744, 3-(2-hydroxyethyl)-2-[2-[[3-(2-hydroxyethyl)-5-methoxy-2-benzthiazolylidene]methyl]-1-butenyl]-5-methoxybenzothiazolium; C11, 3,3′-diethyl-9-methyl-thiacarbocyanine iodide;

utilizing *in vitro* assays (25–27). N744 was capable of inhibiting filament formation at substoichiometric concentrations with an IC_{50} of 294 ± 23 nM (25). Analysis utilizing electron microscopy revealed that N744 was capable of reducing both total filament mass and filament number. Also, substoichiometric concentrations of N744 were capable of disaggregating mature filaments. Over 19 h of incubation total filament length was reduced to 13 ± 2% of the control (25). In contrast to other polymerization inhibitors, length distribution remained unchanged with N744 treatment. This is not inconsequential as these results indicate that disaggregation was endwise rather than the result of random breakage. Interestingly, further study revealed that N744 activity is biphasic with optimal inhibition occurring at ~4 μM (26). Above this concentration, inhibition is relieved and polymerization levels greater than control samples are observed at higher drug concentrations. These changes are reflected by changes in the equilibrium constant, or minimal concentration, for Tau polymerization. In the inhibitory range, increasing doses of N744 produced corresponding increases in the critical concentration. In contrast, higher concentrations of N744 resulted in a lowering of the equilibrium constant. Although N744 is not capable of directly triggering Tau polymerization, it appears capable of increasing the concentration of Tau available for incorporation into fibrils by competitively binding to the negatively charged surfaces presented by polymerization inducers (26). These findings demonstrate the potential usefulness of cyanine dyes as candidates for development as therapeutics and use in hypothesis testing.

Within the cyanine dye family, there are multiple commercially available molecules that vary with respect to the meso substituent, bridge length, and N substituent. Of these, 3,3′-diethyl-9-methylthiacarbocyanine iodide (C11) was found to have a similar potency *in vitro* to N744 (28). In addition, the molecular properties of C11 present distinct advantages compared with N744. Comparisons of topological polar surface area, octanol water partition coefficient (miLogP), and molecular weight indicate that C11 is more likely to cross the blood-brain barrier, and thus was chosen for further study.

Here we examine the effects of cyanine dye C11 over a wide concentration range in a transfected cell and an *ex vivo* culture system making aggregated, tangle-type Tau. An inactive cyanine, C2, was used to control for nonspecific effects of the cyanine scaffold. Two different culture systems were utilized to assay the effects of cyanine treatment on Tau polymerization. In the first, organotypic slices were cultured from the hTau mouse line that expresses all six isoforms of wild type human Tau. Slice cultures accumulate a robust level of aggregated Tau in a physiologically relevant milieu. In addition, because the hemispheres are plated separately, one hemisphere may be retained to serve as a within-animal control, thus eliminating the problem of variable aggregate levels between animals. A second culture system utilized human embryonic kidney cells transfected with split GFP-labeled Tau. In this assay, GFP fluorescence is altered upon Tau aggregation with higher degrees of polymerization resulting in reduced GFP signal (29). This system allows for a high number of replicates as well as fast and quantitative measurements. Results show that C11 is capable of significantly reducing levels of aggregated Tau at submicromolar concentrations (0.001 μM) with no effects on polymerization with C2. In addition, these effects were not dependent on changes in phosphorylation state.

PARP, poly(ADP-ribose) polymerase; DMSO, dimethyl sulfoxide; GFP, green fluorescent protein; MES, 4-morpholineethanesulfonic acid.

EXPERIMENTAL PROCEDURES

Animals—To generate the hTau line, transgenic mice (line 8c (30)) were crossed to a targeted line in which the endogenous mouse Tau gene was non-functional (31). Pups at postnatal day 10 from the hTau mouse line (32) of either sex were utilized for organotypic slice cultures. The hTau line expresses all six isoforms of human wild-type Tau under the control of the human Tau promoter due to integration of a PAC-derived human genomic sequence. Animals were used in accordance with National Institute of Health/Institutional Animal Care and Use guidelines.

Antibodies—The following monoclonal anti-Tau antibodies were used, CP27 (total human Tau) and PHF-1 (phospho-$Ser^{396/404}$) were gifts from Dr. Peter Davies (Albert Einstein, New York, NY). AT8 (phospho-$Ser^{202/205}$) and phospho-Thr^{212} monoclonal antibody were purchased from Thermo (Rockford, IL). Phospho-Ser^{262} and phospho-Ser^{396} were obtained from BIOSOURCE (Camarillo, CA). Monoclonal anti-α-tubulin and synaptophysin antibodies were purchased from Sigma. Anti-cleaved poly(ADP-ribose) polymerase (PARP) antibody was obtained from Cell Signaling (Danvers, MA).

Preparation of Organotypic Slices—Organotypic slice cultures were prepared utilizing protocols modified from Duff *et al.* (33) (depicted in Fig. 1). Brains were removed from hTau pups at postnatal day 10. Hemispheres (cortex and hippocampus) were sectioned into 400-μm thick slices and separated in ice-cold buffer (pH 7.1). Slices (~18 per hemisphere) were transferred to membrane inserts containing 0.4-μm pores (Laboratory Disposable Products, Wayne, NJ). Following sectioning, slices were allowed to incubate in culture for 14 days in media containing 25% serum. Media was exchanged every 2 days. Following the incubation period slices comprising each hemisphere were treated with either C11 (Sigma, structure shown in Fig. 2) or DMSO vehicle (final concentration of DMSO in media 0.008%), thus allowing the DMSO-treated slices to serve as a within-animal control. C11-treated slices were dosed at 1.0, 0.1, or 0.001 μM ($n = 6$ mice per group). This compound is structurally similar to a previously identified Tau polymerization antagonist N744 and it has a similar dose-response curve *in vitro*. Additional slices ($n = 5$ mice) were treated with either 0.001 μM C2 (an inactive cyanine) or DMSO control (final concentration of DMSO in media 0.008%).

Tissue Fractionation—Tissue fractionation procedures were adapted from Greenberg and Davies (34). Control and C11- or C2-treated slices were homogenized in RIPA buffer (50 mM Tris-HCl, pH 7.4, 150 mM NaCl, 1 mM EDTA, 1 mM sodium fluoride, 1 mM Na_3VO_4, 1 μg/ml protease inhibitors, 1 μg/ml phosphatase inhibitors) and centrifuged at 20,000 × *g* for 20 min at 4 °C. The pellet fraction was discarded and the resulting supernatant assayed for total protein concentration. Samples were then diluted as necessary to achieve equivalent total pro-

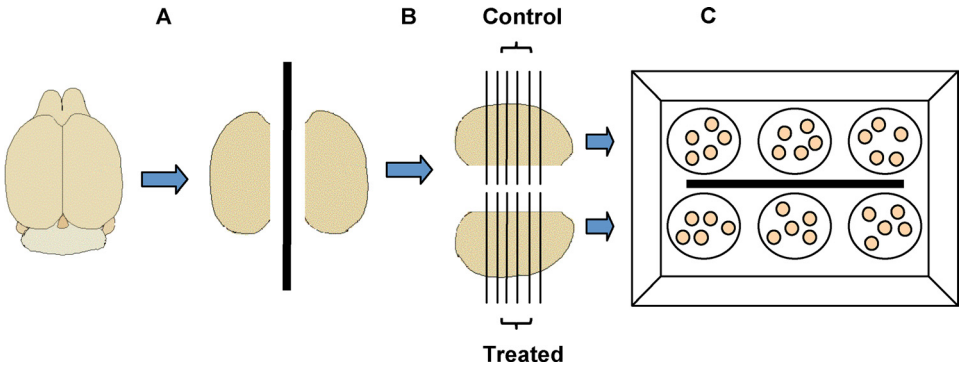

FIGURE 1. **Preparation of organotypic slices.** *A*, brains were removed from hTau pups between 9 and 11 days postnatal. Olfactory bulb and brainstem are removed and the hemispheres (cortex/hippocampus) were separated. *B*, each hemisphere was sectioned into 400-μm slices. *C*, slices from each hemisphere were plated in tissue culture inserts on different rows in six well plates. This method allows each animal to act as its own control thus eliminating the problem of variability due to differing pathology between individual animals.

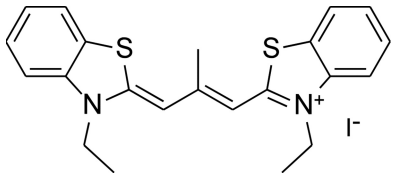

FIGURE 2. **Structure of cyanine dye C11.**

tein levels. To generate the heat stable (S) fraction an aliquot of the low speed supernatant was retained and boiled for 10 min. After heating, the samples were centrifuged at 20,000 × *g* for 20 min at 4 °C and the supernatant was retained and diluted in O+ buffer (62.5 mM Tris-HCl, pH 6.8, 5% glycerol, 2-mercaptoehtanol, 2.3% SDS, 1 mM EGTA, 1 mM phenylmethylsulfonyl fluoride, 1 mM $NaVO_4$, 1 μg/ml protease inhibitors, 1 μg/ml phosphatase inhibitors). The S fraction represents soluble Tau. To isolate Tau polymers, an additional fraction of low speed supernatant was incubated in 1% Sarkosyl for 30 min at room temperature. Samples were then centrifuged for 1 h at 100,000 × *g* at 20 °C. Supernatant was discarded and the Sarkosyl-insoluble pellet was resuspended in 20 μl of O+ buffer.

Estimation of C11 Concentration—Because the effects of C11 are mediated by dye concentration, determining the level of compound in the target tissue may explain the observed effects on Tau polymerization. Slices were washed three times in phosphate-buffered saline to remove dye bound to the surface of the tissue. Slices were then collected as described above and centrifuged at 20,000 × *g* for 20 min at 4 °C. Supernatant fractions were removed and reserved for determination of C11 concentration. To generate a standard curve, varying concentrations of C11 (0.001–10 μM) were incubated in untreated tissue homogenates overnight at 37 °C in a 96-well plate. Following incubation, homogenates from control and treated samples were added to the plate in triplicate. Fluorescence data were collected using a TECAN Infinite M200 plate reader, excitation 550 nm, emission 585 nm (35). Average and standard deviation for each sample and standard was calculated. The average fluorescence of each standard was then plotted against the C11 concentration to generate a standard curve. Slope of the resultant line was determined and utilized to estimate dye concentration in the treated samples.

Preparation of Samples for Electron Microscopy—Sarkosyl-insoluble fractions from control and treated slices were prepared as described above with the exception that the final pellet was resuspended in 100 μl of phosphate-buffered saline. Samples were fixed with glutaraldehyde (2% final volume) and adsorbed onto 400-esh formvar-coated copper electron microscope grids (Electron Microscopy Sciences, Ft. Washington, PA) for 20 min. Grids were then washed with double distilled water. Grids were then stained with uranyl acetate (Electron Microscopy Sciences) at 2% final volume for 5 min. Following staining, grids were washed a second time.

Microtubule Binding Assay—Because C11 is capable of binding to the Tau protein it is important to ascertain whether the presence of the drug interferes with normal microtubule binding, which is potentially detrimental. Additional slices were prepared and treated as described above with either 1.0 or 0.001 μM C11. Microtubule binding assays were conducted utilizing methods adapted from Volgelsberg-Ragaglia (36). Samples were homogenized in warm (37 °C) RAB buffer (0.1 M MES, pH 6.8, 0.5 mM $MgSO_4$, 1 mM EGTA, 1% Triton X-100, 20 μM Taxol, 2 mM GTP, phosphatase inhibitor mixture, and protein inhibitor mixture) using a warmed Dounce homogenizer. Samples were centrifuged at 3,000 × *g* for 4 min at 25 °C to remove debris. The resulting supernatant was collected and a 50-μl aliquot was diluted in O+ buffer and boiled for 5 min. A 100-μl aliquot of the remaining supernatant was centrifuged at 100,000 × *G* for 20 min at 25 °C. The supernatant was collected and the pellet was resuspended in 100 μl of RAB buffer. Fifty-μl fractions of both the supernatant and pellet fractions were diluted in 450 μl of O+ buffer and boiled. Immunoblotting was carried out on the total, cytosolic (free), and microtubule-bound fractions with CP27 as the primary antibody.

Quantitative Immunoblot Analysis—Membranes were blocked for 30 min in phosphate-buffered saline containing 5% milk. Appropriate dilutions of primary and secondary antibodies were applied. Bands were visualized with enhanced chemiluminescence reagent (Immunobilon Western HRP substrate luminol reagent, Millipore) using a Fujifilm LAS3000 imaging system in the linear range. Signal was quantified using Multigauge version 3.0.

Filament Quantification—Random images from each grid were obtained using a JEOL 1200 transmission electron microscope operated at 80 kV at ×12,000 magnification. Images were imported into Image J and individual filaments were traced manually to obtain length data. These methods have been well established in multiple *in vitro* studies (37–39). Total length and filament number were averaged over each condition and standard deviation calculated. For each image the total number of filaments in each 10-nm length range, or bin, was determined

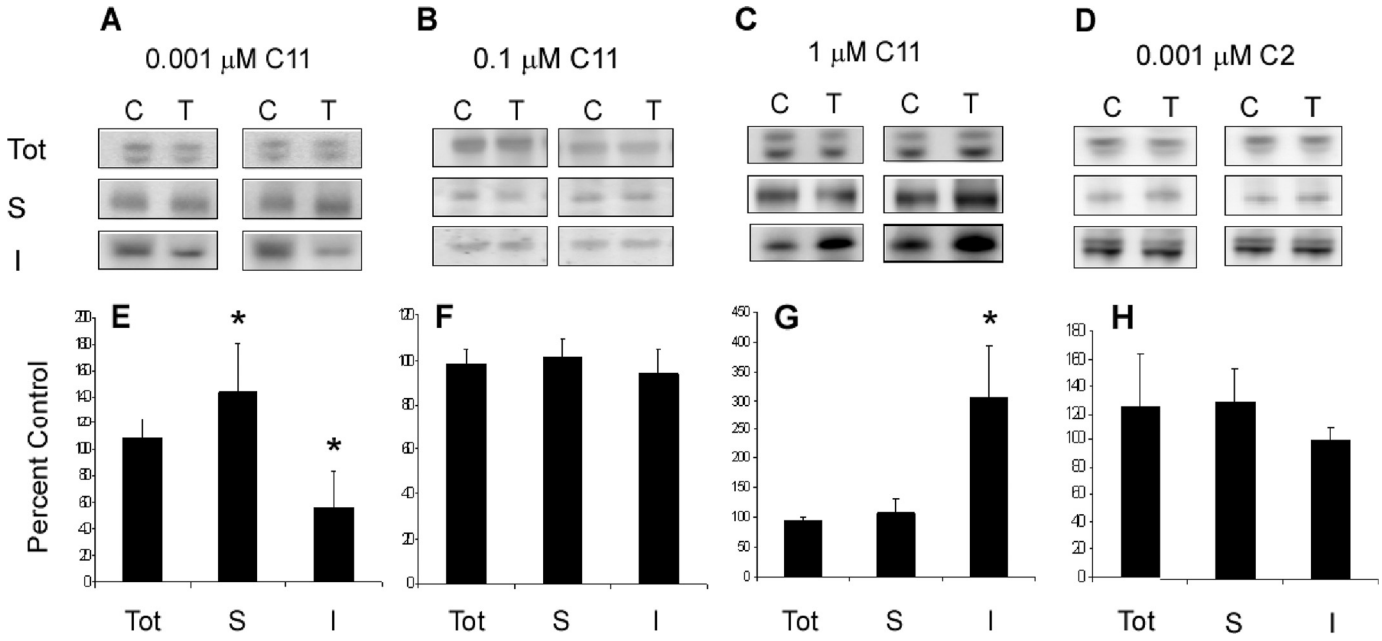

FIGURE 3. **C11, but not C2 treatment modulates Tau polymerization.** Slice cultures were treated as described with 0.001, 0.1, and 1 μM C11 ($n = 6$ per group) or 0.001 μM C2 ($n = 5$). *A–D,* immunoblotting was carried out on the total (*Tot*), soluble (*S*), and Sarkosyl-insoluble (*I*) fractions. Blots were incubated with CP27, a monoclonal antibody recognizing all six human Tau isoforms, and bands were visualized. Images were quantified using Multigauge version 3.0 and expressed as percentage of control signal ± S.E. *E,* following treatment with 0.001 μM C11, total Tau levels remained unchanged (107.6 ± 15.7). Soluble Tau levels increased to 112 ± 9% control ($p = 0.01$). Sarkosyl-insoluble Tau was reduced to 55.5 ± 27.7% of that of control slices ($p = 0.003$). *F,* slices dosed with 0.1 μM showed no change in levels of total (98.03 ± 6.8) soluble (101.3 ± 7.9) or aggregated (94.1 ± 10.6) Tau. *G,* incubation with 1 μM C11 resulted in no change in total (94.1 ± 6.53) or soluble (108 ± 22.5) Tau levels relative to control. Insoluble Tau levels increased ($p = 0.001$) with treatment (305.43 ± 86.9). *H,* the inactive cyanine C2 showed no changes in the levels of total, soluble, or insoluble Tau relative to control slices. * indicates $p < .05$.

and expressed as a percentage of total filament number. The percentage of filaments per bin was then averaged and plotted against length interval midpoint.

Plasmid Construction—Plasmids were generated as previously described (29). Briefly, the small fragment of GFP was amplified by PCR and cloned into XbaI and ApaI sites of *pcDNA3.1*(+). *pcDNA3.1*(−)*-T4* was used to generate human Tau isoform 24 (containing exon 10 but lacking exons two and three). To obtain Tau-GFP_{11}, Tau PCR products were cloned into the KpnI and XbaI sites of the *pcDNA3.1*(+) with the GFP vector. The large GFP fragment was cloned into the NheI and NotI sites of *pcDNA3.1*(−).

Cell Culture—Human embryonic kidney cells were grown in clear bottom 96-well plates in Opti-MEM (Cellgro, Herndon, VA) with media exchanged every other day. Cells were allowed to incubate in culture for either 1 or 2 days post-transfection following which they were treated with either C11 or DMSO vehicle (DMSO final concentration in media, 0.3%).

Detection of GFP and C11—GFP complementation was measured daily using a TECAN Infinite M200 plate reader with an excitation wavelength of 485 nm and an emission wavelength of 520. C11 fluorescence was measured concurrently. Signal was averaged over wells in each condition ($n = 8$) and plotted as percent of initial value against time.

Analytical Methods—Chemiluminescence signal was determined as described above. For each sample, signal relative to control was determined for each treated samples. Average and standard error was determined for each group. Statistical significance was determined utilizing a two-tailed Student's *t* test.

RESULTS

C11 but Not C2 Is Capable of Modulating Tau Polymerization in Organotypic Slice Cultures—Tissue fractionation was performed as described above for slices ($n = 6$ mice per group) treated with C11, C2, and vehicle control. All fractions were subjected to immunoblotting with CP27, an antibody against human Tau (Fig. 3). No significant change in total Tau levels was observed in any C11 dosing regime (107.6 ± 15.7 for 0.001 μM, 98.03 ± 6.4 for 0.1 μM, and 94.1 ± 6.53 for 1 μM C11) relative to control. In addition, no change was seen in the levels of Tau in the soluble fraction relative to control in slices treated with 0.1, or 1 μM C11 (94.1 ± 10.6 and 108.1 ± 22.5). However, treatment with 0.001 μM C11 resulted in a significant increase ($p = 0.01$) in soluble Tau. This increase in unpolymerized Tau is mirrored by a reduction in the levels of aggregated protein. Addition of 0.001 μM C11 to culture media produced a significant reduction ($p = 0.003$) in Sarkosyl-insoluble Tau relative to untreated slices from the same animal (55 ± 27.7). In contrast, incubation with 1 μM C11 resulted in significantly elevated ($p = 0.001$) levels of polymerized Tau (305.43 ± 86.9). No change was observed in slices treated with 0.1 μM (101.3 ± 7.9). These results indicate that the biphasic effects observed with cyanine dyes incubated with recombinant Tau *in vitro* are also present in cultured tissue (26). However, compared with *in vitro* studies, much lower doses were required to achieve inhibition. Because 1 μM and 0.001 μM doses produced significant and opposing effects on Tau polymerization, they were chosen for further investigation. No change in the concentration of aggregated Tau was observed following treatment with compound

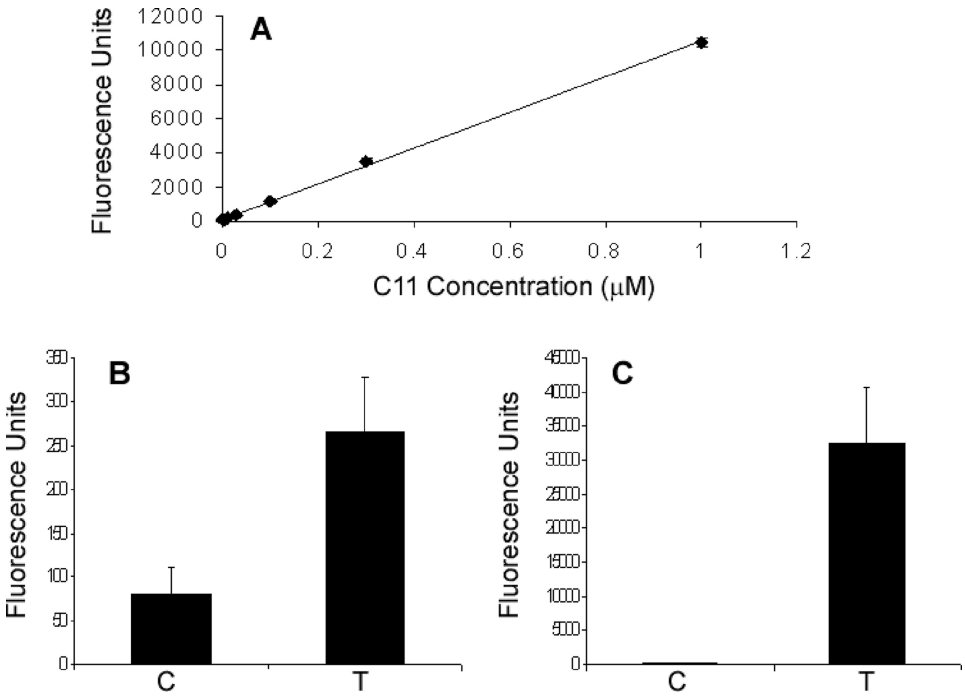

FIGURE 4. **C11 is internalized and concentrated in slice cultures.** *A*, untreated homogenate was incubated in triplicate for 24 h at 37 °C with varying (1.0–0.003 μM) concentrations of C11. Fluorescence signal was then plotted against C11 concentration and a linear curve fit to the data ($y = 10442x \pm 128.17$). *B*, in 0.001 μM treated (*T*) and control (*C*) slices ($n = 6$ mice per group) fluorescence was 183 ± 61.7 and 80.2 ± 33.3, respectively. *C*, average fluorescence was measured in homogenates ($n = 6$ per group) of 1 μM C11 treated (*T*) and control (*C*) slices. Values obtained were 32,504.8 ± 8,212.9 and 153.8 ± 38.9, respectively. Utilizing the equation of the standard curve, the C11 concentration in 1 μM and 0.001 μM treated samples was estimated as 3.1 and 0.0053 μM, respectively.

C2, indicating that the compound is ineffective against Tau polymerization in culture as well as in recombinant protein.

C11 Is Detectable in Slice Homogenate—Fluorescence measurements were obtained in triplicate for each standard, control, and treated sample. Values recorded from the standard samples were averaged and plotted against C11 concentration to generate the standard curve (Fig. 4*A*). The equation for the resultant line was calculated as,

$$y = 10442x + 128.17 \quad \text{(Eq. 1)}$$

with an R^2 value of 0.991. Average fluorescence was then calculated for each of the control and treated samples with values of 32,504 ± 8,212.9 and 183.2 ± 61.7 for 1 μM (Fig. 4*B*) and 0.001 μM (Fig. 4*C*), respectively. Utilizing Equation 1, the concentration of C11 in treated slices was estimated as 0.0053 and 3.101 μM for the 0.001 and 1 μM dosing regimes, thereby indicating that the drug is taken up and concentrated by the tissue.

Changes in Tau Polymerization Are Not Dependent on Changes in Phosphorylation—Because hyperphosphorylation has been postulated as a polymerization promoter (40–43) and multiple aggregation inhibitors act via effects on protein kinases (44–46), an examination of whether C11 also affects phosphorylation was performed. The heat-stable fraction from control, C11-, and C2-treated slices were subjected to immunoblotting to assay for changes in phosphorylation state (Fig. 5*A*). However, no changes in occupancy were seen in either C11 dosing regime or with C2 treatment at $Ser^{202/205}$ (AT8), Thr^{212}, Ser^{262}, Ser^{396}, or $Ser^{396/404}$ (PHF-1) sites (Fig. 5, *B–F*). These sites have been implicated in disease or as modulators of polymerization *in vitro*. These data demonstrate that Tau polymerization can be targeted independently of phosphorylation. As Tau kinases have multiple targets within the cell, directly targeting abnormal Tau may provide a way to reduce the unwanted side effects of treatment.

C11 Modulates Both Total Filament Mass and Number but Does Not Affect Length Distribution—Well characterized electron microscopy methods were utilized to assay the effect of C11 treatment at the level of individual filaments. Individual filament lengths were quantified using the Image J program and total filament length and number were determined for each grid and expressed as percent control. Treatment with 0.001 μM C11 resulted in a significant decrease ($p = 0.01$) in filament number relative to control. In contrast, average filament number significantly increased ($p = 0.01$) to 207.96% of control following incubation with 1 μM C11 (Fig. 6*A*). Similar to filament number, at 0.001 μM C11 average total filament length was significantly reduced ($p < 0.001$) to 23.63% of total length obtained from control slices. In addition, significantly higher ($p < 0.001$) total filament mass at the time of tissue collection was achieved with the higher dose (317.1% compared with control slices) (Fig. 6*B*). No significant change was seen in the filament length distribution at either dose (Fig. 6, *C* and *D*). In both dosing regimes, the distribution was exponential for control and treated samples. This suggests that changes in filament mass and number are not the result of random breakage. This is not insignificant as breakage may produce further nucleation sites.

C11 Treatment Does Not Affect Slice Viability—Additional immunoblots were performed to assess the effect of C11 treatment on slice viability, synaptic, and cytoskeletal integrity (Fig. 7). No changes were seen in levels of cleaved PARP indicating that C11 treatment at either dose does not result in activation of pro-apoptotic caspases (90.9 ± 28.4 for 0.001 μM and 90.04 ± 21.1 for 1 μM). Similarly, in both dosing regimes, no significant change in the level of synaptophysin immunoreactivity was detected (117.3 ± 26.5 for 0.001 μM and 92.2 ± 26.6 for 1 μM). Tubulin levels were likewise unchanged in cultures incubated with 0.001 μM C11 (103.4 ± 25.8). However, when dosed with 1 μM, a significant reduction in tubulin concentration was detected (20.4 ± 22.7). Additional immunoblots from the Sarkosyl-insoluble fraction of Tau revealed the presence of tubulin at significantly higher levels relative to control samples (data not shown). This result suggests that the increased Tau polym-

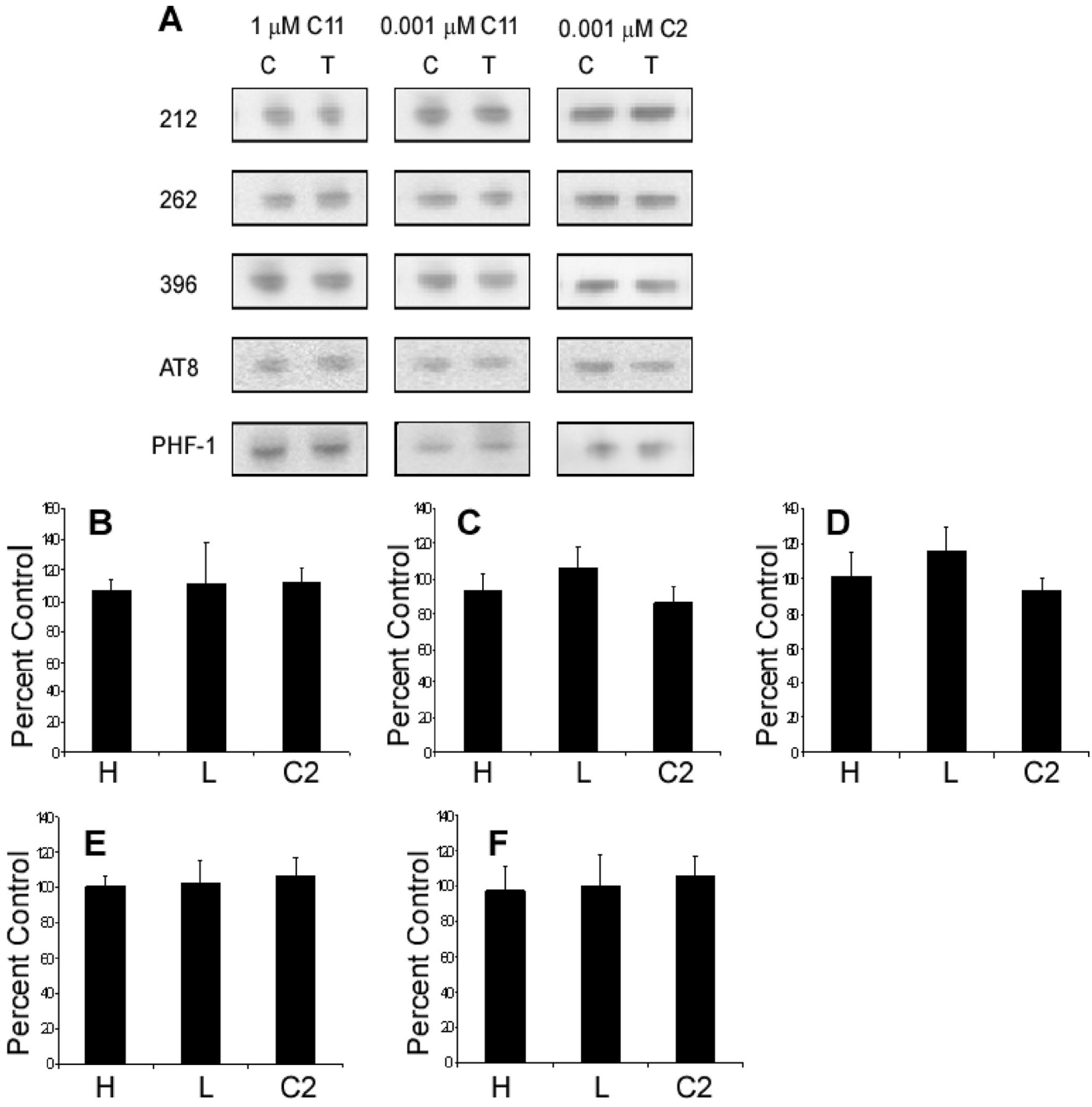

FIGURE 5. **Incubation with C11 does not affect phosphorylation.** *A*, aliquots from the heat stable fraction of control (*C*) and treated (*T*) slices were used to determine the relative levels of phosphorylation at disease and polymerization relevant epitopes. *B–F,* immunoblots were processed and quantified as described. No changes were seen in band intensity or mobility relative to control for Thr^{212} (*B*) (106.3 ± 7.6 for 1 μM (*H*), 111.02 ± 26.4 for 0.001 μM (*L*), and 112.2 ± 9.6 for C1), Ser^{262} (*C*) (93.2 ± 9.6 for 1 μM, 106.1 ± 12.3 for 1 μM, and 86.9 ± 8.6 for C1), Ser^{396} (*D*) (101.2 ± 13.7 for 1 μM, 116.6 ± 13.5 for 0.001 μM, and 93.8 ± 6.7 for C1), AT8 (*E*) (100.8 ± 5.3 for 1 μM, 102.8 ± 12.6 for 0.001 μM, and 106.4 ± 10.62 for C1), or PHF-1 (*F*) (97.8 ± 13.8 for 1 μM, 100.04 ± 18.03 for 0.001 μM, and 106.4 ± 10.6 for C1).

erization observed following high dose C11 treatment results in tubulin being sequestered into the intracellular Tau aggregates.

Inhibitory Doses of C11 Do Not Affect Microtubule Binding—Because C11 is capable of binding Tau, it is necessary to assess whether this binding interferes with the ability of the protein to interact with tubulin. Slices were treated as described above with either 1 or 0.001 μM C11 *versus* DMSO vehicle (Fig. 8). Again, total Tau levels relative to control remained unchanged (91.1 ± 8.6 for 1 μM and 104.4 ± 11.8 for 0.001 μM). When incubated with 0.001 μM, treated slices showed no change in the ratio of microtubule bound (93.5 ± 12.9) and unbound Tau (94.1 ± 11.7). Indeed, the majority of Tau in the cells was microtubule bound with only faint immunoreactivity in the unbound supernatant fraction. These results indicate that at submicromolar concentrations, C11 does not appear to affect normal Tau-microtubule interaction. In contrast, addition of 1 μM C11 to the culture media resulted in a significant shift in the pattern of Tau binding with treated slices, showing marked microtubule detachment relative to control slices. This is

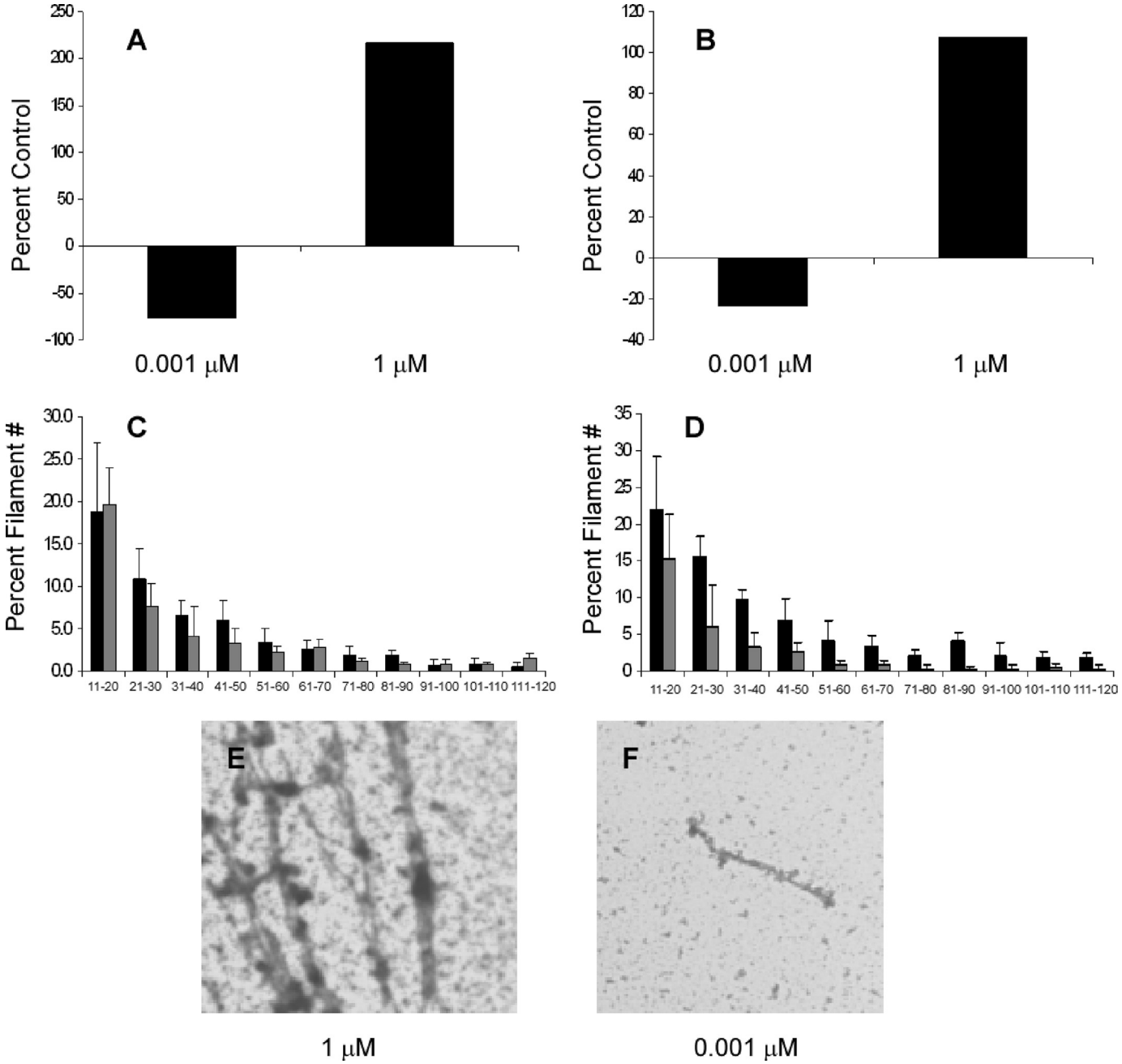

FIGURE 6. **C11 treatment results in changes in filament mass and number.** Filaments in the Sarkosyl-insoluble fraction were negatively stained with uranyl acetate. Image J was used to measure total filament length obtained for each electron micrograph and the average for each condition was calculated. *A,* total filament number as a percentage of control was determined. A significant increase ($p = 0.01$) was observed at 1 μM (207.96%), whereas treatment with 0.001 μM produced a significant decrease ($p = 0.01$) (76.24% of control) *B,* significantly higher ($p < 0.001$) total filament mass was observed at 1 μM C11 (317.1% of control). In contrast, 0.001 μM treated samples showed a significant reduction ($p < 0.001$) to 23.63% of control values. *C* and *D,* the number of filaments falling into each 10-nm length range was determined and expressed as a percentage of total filament number. Distributions were similar for control (*black bars*) and treated (*gray bars*) samples. *E* and *F*, electron micrographs from 1 μM and 0.001 μM treated samples, respectively, are shown.

unsurprising considering the sequestration of tubulin with Tau aggregates at this dose.

C11 Alters Tau Polymerization in Split GFP Tau-transfected Cells—Following transfection, cells were incubated overnight prior to addition of C11. GFP fluorescence steadily decreased in both untreated controls and cells dosed with 1 μM C11 (Fig. 9). However, both the rate and extent of the decrease was augmented in response to high dose C11. A 50 $\pm$ 0.97% reduction if GFP fluorescence (from 35,993 fluorescence units to 18,460) was observed in control cells after 3 days in culture, reflecting the increase in Tau aggregates. Cells treated with 1 μM C11 showed a 62 $\pm$ 1.27% loss of GFP signal (from 32,065 to 12,326) reflecting a significantly greater degree of Tau aggregation relative to control. Indeed, at each time point, treated cells showed significantly reduced fluorescence ($p < 0.001$) suggesting accelerated aggregate formation. To ascertain whether treatment with low concentrations of C11 reduced Tau polymerization, cells were allowed to incubate without treatment for 2 days in culture to accumulate aggregates. C11 was then added to the media and cells were incubated with the drug for a further 2

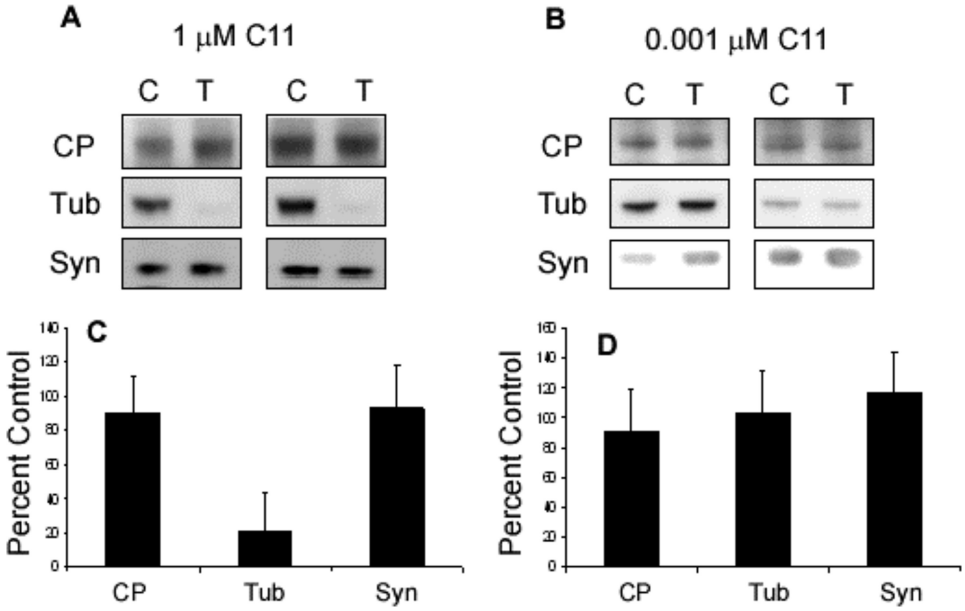

FIGURE 7. **C11 treatment does not negatively affect slice viability.** Total protein fractions were assayed for relative levels of cleaved PARP, tubulin, and synaptophysin to ascertain the health of the cultures. *A* and *C*, slices incubated with 1 μM C11 showed no difference in cleaved PARP (*CP*) (92.2 $\pm$ 26.5) or synaptophysin (*Syn*) (90.04 $\pm$ 21.1) signal relative to control, however, a marked decrease in tubulin (*Tub*) immunoreactivity was observed (44.5 $\pm$ 27.5). *B* and *D*, no changes in the relative concentration of any of the proteins was observed with 0.001 μM C11 (90.9 $\pm$ 28.4 for cleaved PARP, 117.3 $\pm$ 26.5 for synaptophysin (*Syn*), and 103.8 $\pm$ 28.5 for tubulin (*Tub*)).

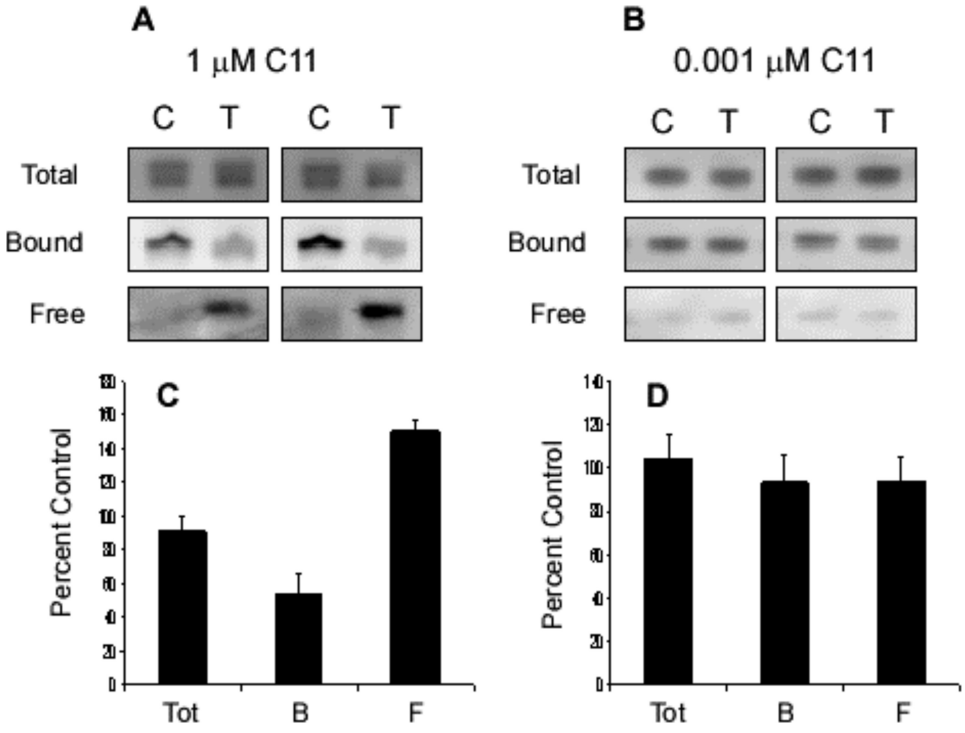

FIGURE 8. **High dose, but not low dose C11 treatment affects microtubule binding.** An assay of Tau-microtubule binding was performed. Total, microtubule-bound and unbound (free) Tau was assessed by immunoblotting. *A* and *C*, following incubation with 1 μM C11 no change in the level of total Tau (91.1 $\pm$ 8.6) was observed. However, a decrease in microtubule-bound (53.8 $\pm$ 12.6) and an increase in free Tau (150.9 $\pm$ 5.8) was found compared with DMSO-treated controls. *B* and *D*, no change in the relative concentration of total (*Tot*) (104.4 $\pm$ 11.8), microtubule-bound (*B*) (93.5 $\pm$ 12.9), or free (*F*) Tau (94.06 $\pm$ 11.7) was observed with 0.001 μM C11.

days. Following treatment, fluorescence was measured. As before, fluorescence decreased progressively in control cells with a final value of 78 $\pm$ 2.7% of control (from 34,854 to 27,327). Significantly higher fluorescence was obtained in 0.01 μM treated cells relative to control. Indeed, incubation with the drug for 3 days resulted in no significant loss of GFP signal, indicating that polymerized Tau did not accumulate at this dose. These data indicate a shift of the dose-response curve in different culture systems. However, although the inhibitory dose differs, in both systems 1 mM C11 led to increased aggregation. In the organotypic slices 0.001 μM was the optimal dose whereas, in cells a 10-fold higher dose was required to prevent polymerization. However, both values are markedly lower than the IC_{50} of ~280 μM obtained *in vitro*.

DISCUSSION

Insoluble Tau polymers accumulate in affected cells in a host of neurodegenerative conditions. Identification of compounds capable of reducing the burden of aggregated Tau could potentially result in the creation of disease-modifying therapies. One such example, methylthioninium chloride (methylene blue, Rember^{TM}), which has been shown to reduce Tau fibrillization *in vitro* (24, 47), is the subject of clinical trials.

In vitro studies have shown that small molecule cyanine dyes are capable of selectively binding to abnormally folded Tau protein and modulating its polymerization in a biphasic, dose-dependent manner (25). We have shown that it is possible to recapitulate these results in an organotypic slice culture system. Cyanine dye C11 is capable of either significantly reducing, or increasing the levels of Sarkosyl-insoluble Tau. Indeed, inhibition is possible at submicromolar concentrations without affecting normal microtubule binding or adverse effects on synaptic integrity. As a control, a similar molecule (C2) determined to be inactive *in vitro* was utilized to assess nonspecific effects of the cyanine skeleton. No changes were seen in the relative amounts of total, soluble and polymerized Tau relative to untreated slices. Furthermore, no changes were seen in tubulin, synaptophysin, or cleaved PARP with C2 treat-

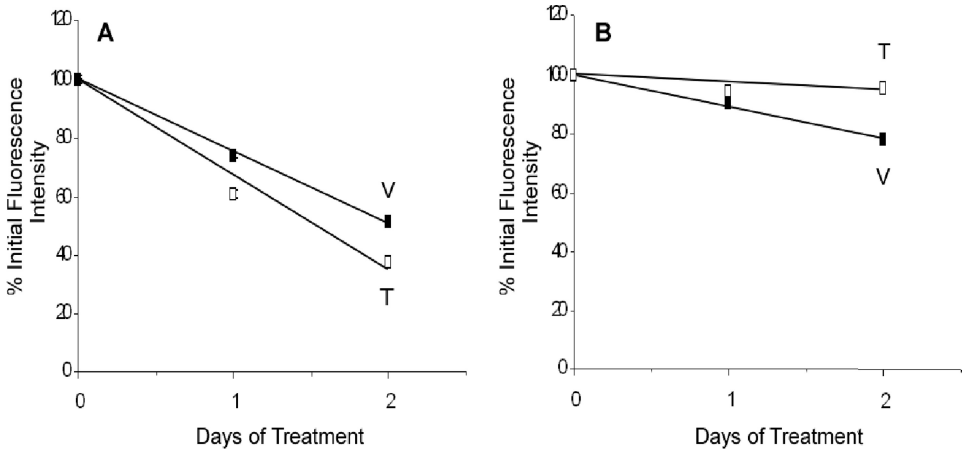

FIGURE 9. **C11 treatment alters Tau polymerization in a cellular, Tau aggregation assay system.** *A*, GFP-Tau-transfected human embryonic kidney cells were incubated in culture for 24 h. Cells were then incubated with either DMSO vehicle (■) or 1 μM C11 (□) for a further 2 days. Fluorescence in control cells decreased 50 ± 0.97% during incubation (from 35,993.8 fluorescence units to 18,011.8). However, drug treatment resulted in a 62 ± 1.27% decrease in fluorescence (from 32,696.4 to 12,326.1 units), indicating that 1 μM C11 significantly increased Tau polymerization. *B*, cells were allowed to incubate in culture for 2 days prior to treatment to accumulate polymerized Tau. Following this, cells were treated with either DMSO vehicle (■) or 0.01 μM C11 (□). Fluorescence in vehicle-treated cells decreased 22 ± 2.78% from 34,854 to 27,237. In contrast, treated cells demonstrated no significant loss of signal (35,436 to 33,835).

ment. In addition, effects on polymerization were not dependent on alterations in Tau phosphorylation, indicating that a reduction in occupancy at phosphoepitopes is not required to reduce Tau filament burden. These results also suggest that increased levels of soluble, hyperphosphorylated Tau monomers are not toxic to the slice cultures. However, at present, slices have only been incubated with C11 for 1 week in culture. It may require longer periods of incubation, or additional assay methods for toxicity to become apparent. Furthermore, these results have been confirmed using a second model system. In these studies, low doses of C11 were capable of significantly reducing the levels of aggregated Tau in cells transfected with the longest human Tau isoform.

In contrast, treatment with 1 μM C11 produced a significant elevation of polymerized Tau with a marked decrease in the levels of soluble tubulin. This was accompanied by an increase in tubulin in the Sarkosyl-insoluble fraction. Studies utilizing N744 suggest that a possible mechanism by which cyanine dyes facilitate Tau polymerization is through competitive binding. Dye polymers were capable of displacing Tau from the surface of negatively charged polystyrene microspheres and thus raising the concentration of Tau in solution. A similar process may be occurring in the slice cultures. Incubation with higher doses of C11 may result in the displacement of Tau from the microtubule surface. This would result in an increase in the concentration of Tau available for incorporation into aggregates. Additionally, previous studies have shown that several microtubule-associated proteins such as microtubule-associated proteins 1 and 2 can be sequestered into neurofibrillary lesions and the Sarkosyl-insoluble fraction. It may be that additional microtubule-associated proteins are also being recruited into the Sarkosyl-insoluble fraction and this loss of support results in the destabilization of the microtubules. This destabilization could then allow tubulin dimers to be likewise sequestered in the Sarkosyl-insoluble fraction. Loss of tubulin and increased Tau filament burden does not, however, appear to result in increased toxicity after 1 week. No loss of synaptic integrity or activation of pro-apoptotic caspases was observed. On a superficial level, slices treated with 1 μM C11 did not appear less healthy than control, neutral, or low dose-treated cultures. As stated above, longer incubation times may be necessary to observe toxic effects. Further studies will be necessary to fully evaluate the consequences of altered Tau polymerization.

Similar to N744, the dose-response relationship of C11 indicates the existence of a therapeutic index. Among compounds that act on amyloid-forming proteins, this is not unheard of. A similar dose-response effect was observed with Congo Red in models of Huntington disease. *In vitro*, Congo Red has a monophasic and steep dose-response curve (48). However, in biological models, a more complex pattern emerges. Low concentrations inhibited huntingtin polymerization with higher doses resulting in relief of that inhibition (49). Similarly, although it retains its biphasic shape, the dose-response curve of C11 shifts depending on the model system utilized. Although this may limit the utility of C11, it should be noted that a 100–1000-fold increase in concentration is required to promote Tau aggregation. Additionally, these results indicate that results obtained in animals or tissue culture with aggregation inhibitors identified *in vitro* must be interpreted carefully. Indeed, what may appear to be a negative result may in fact occur because the dose-response curve has shifted due to changing model systems. This may result in promising compounds being abandoned unnecessarily.

Finally, these findings further demonstrate the potential utility of cyanine dyes. This class of molecules has also been successfully used in cell culture as inhibitors of nitric oxide production (50). In addition, a cyanine dye, Platonin, has been shown to reduce tissue damage and improve survival in a rat model of heat stroke (51). Cyanines have also demonstrated utility as contrast agents (52, 53) and one, Cardio Green, has been approved for use in humans. Together with the results described above, these data indicate the potential of this class of compounds for further development as potential therapies.

REFERENCES

1. Farah, C. A., Perreault, S., Liazoghli, D., Desjardins, M., Anton, A., Lauzon, M., Paiement, J., and Leclerc, N. (2006) *Cell Motil. Cytoskeleton* **63,** 710–724
2. Magnani, E., Fan, J., Gasparini, L., Golding, M., Williams, M., Schiavo, G., Goedert, M., Amos, L. A., and Spillantini, M. G. (2007) *EMBO J.,* **26,** 4546–4554
3. Braak, H., Alafuzoff, I., Arzberger, T., Kretzschmar, H., and Del Tredici, K. (2006) *Acta Neuropathol.* **112,** 389–404

4. Braak, H., and Braak, E. (1991) *Acta Neuropathol.* **82,** 239–259
5. Giannakopoulos, P., Herrmann, F. R., Bussiere, T., Bouras, C., Kovari, E., Perl, D. P., Morrison, J. H., Gold, G., and Hof, P. R. (2003) *Neurology* **60,** 1495–1500
6. Gomez-Isla, T., Hollister, R., West, H., Mui, S., Growdon, J. H., Petersen, R. C., Parisi, J. E., and Hyman, B. T. (1997) *Ann. Neurol.* **41,** 17–24
7. Cras, P., Smith, M. A., Richey, P. L., Siedlak, S. L., Mulvihill, P., and Perry, G. (1995) *Acta Neuropathol.* **89,** 291–295
8. Barghorn, S., Zheng-Fischhofer, Q., Ackmann, M., Biernat, J., von Bergen, M., Mandelkow, E. M., and Mandelkow, E. (2000) *Biochemistry* **39,** 11714–11721
9. von Bergen, M., Barghorn, S., Biernat, J., Mandelkow, E. M., and Mandelkow, E. (2005) *Biochim. Biophys. Acta* **1739,** 158–166
10. von Bergen, M., Barghorn, S., Li, L., Marx, A., Biernat, J., Mandelkow, E. M., and Mandelkow, E. (2001) *J. Biol. Chem.* **276,** 48165–48174
11. Eckermann, K., Mocanu, M. M., Khlistunova, I., Biernat, J., Nissen, A., Hofmann, A., Schonig, K., Bujard, H., Haemisch, A., Mandelkow, E., Zhou, L., Rune, G., and Mandelkow, E. M. (2007) *J. Biol. Chem.* **282,** 31755–31765
12. Callahan, L. M., and Coleman, P. D. (1995) *Neurobiol Aging* **16,** 311–314
13. Hoglinger, G. U., Lannuzel, A., Khondiker, M. E., Michel, P. P., Duyckaerts, C., Feger, J., Champy, P., Prigent, A., Medja, F., Lombes, A., Oertel, W. H., Ruberg, M., and Hirsch, E. C. (2005) *J. Neurochem.* **95,** 930–939
14. Kraemer, B. C., Zhang, B., Leverenz, J. B., Thomas, J. H., Trojanowski, J. Q., and Schellenberg, G. D. (2003) *Proc. Natl. Acad. Sci. U.S.A.* **100,** 9980–9985
15. Callahan, L. M., Vaules, W. A., and Coleman, P. D. (2002) *J. Neuropathol. Exp. Neurol.* **61,** 384–395
16. Chalmers, K. A., and Love, S. (2007) *J. Neuropathol. Exp. Neurol.* **66,** 158–167
17. Bandyopadhyay, B., Li, G., Yin, H., and Kuret, J. (2007) *J. Biol. Chem.* **282,** 16454–16464
18. Khlistunova, I., Biernat, J., Wang, Y., Pickhardt, M., von Bergen, M., Gazova, Z., Mandelkow, E., and Mandelkow, E. M. (2006) *J. Biol. Chem.* **281,** 1205–1214
19. Khlistunova, I., Pickhardt, M., Biernat, J., Wang, Y., Mandelkow, E. M., and Mandelkow, E. (2007) *Curr. Alzheimer Res.* **4,** 544–546
20. Pickhardt, M., Gazova, Z., von Bergen, M., Khlistunova, I., Wang, Y., Hascher, A., Mandelkow, E. M., Biernat, J., and Mandelkow, E. (2005) *J. Biol. Chem.* **280,** 3628–3536
21. Crowe, A., Ballatore, C., Hyde, E., Trojanowski, J. Q., and Lee, V. M. (2007) *Biochem. Biophys. Res. Commun.* **358,** 1–6
22. Pickhardt, M., Biernat, J., Khlistunova, I., Wang, Y. P., Gazova, Z., Mandelkow, E. M., and Mandelkow, E. (2007) *Curr. Alzheimer Res.* **4,** 397–402
23. Pickhardt, M., Larbig, G., Khlistunova, I., Coksezen, A., Meyer, B., Mandelkow, E. M., Schmidt, B., and Mandelkow, E. (2007) *Biochemistry* **46,** 10016–10023
24. Taniguchi, S., Suzuki, N., Masuda, M., Hisanaga, S., Iwatsubo, T., Goedert, M., and Hasegawa, M. (2005) *J. Biol. Chem.* **280,** 7614–7623
25. Chirita, C., Necula, M., and Kuret, J. (2004) *Biochemistry* **43,** 2879–2887
26. Congdon, E. E., Necula, M., Blackstone, R. D., and Kuret, J. (2007) *Arch. Biochem. Biophys.* **465,** 127–135
27. Necula, M., Chirita, C. N., and Kuret, J. (2005) *Biochemistry* **44,** 10227–10237
28. Chang, E., Congdon, E. E., Honson, N. S., Duff, K. E., and Kuret, J. (2009) *J. Med. Chem.*, in press
29. Chun, W., Waldo, G. S., and Johnson, G. V. (2007) *J. Neurochem.* **103,** 2529–2539
30. Duff, K., Knight, H., Refolo, L. M., Sanders, S., Yu, X., Picciano, M., Malester, B., Hutton, M., Adamson, J., Goedert, M., Burki, K., and Davies, P. (2000) *Neurobiol. Dis.* **7,** 87–98
31. Tucker, K. L., Meyer, M., and Barde, Y. A. (2001) *Nat. Neurosci.* **4,** 29–37
32. Andorfer, C., Kress, Y., Espinoza, M., de Silva, R., Tucker, K. L., Barde, Y. A., Duff, K., and Davies, P. (2003) *J. Neurochem.* **86,** 582–590
33. Duff, K., Noble, W., Gaynor, K., and Matsuoka, Y. (2002) *J. Mol. Neurosci.* **19,** 317–320
34. Greenberg, S. G., and Davies, P. (1990) *Proc. Natl. Acad. Sci. U.S.A.* **87,** 5827–5831
35. Petrov, N., Gulakov, M. N., Alfimov, M. V., Busse, G., Frederichs, B., and Techert, S. (2003) *J. Phys. Chem. A* **107,** 6341–6344
36. Vogelsberg-Ragaglia, V., Bruce, J., Richter-Landsberg, C., Zhang, B., Hong, M., Trojanowski, J. Q., and Lee, V. M. (2000) *Mol. Biol. Cell* **11,** 4093–4104
37. Chirita, C. N., Congdon, E. E., Yin, H., and Kuret, J. (2005) *Biochemistry* **44,** 5862–5872
38. Congdon, E. E., Kim, S., Bonchak, J., Songrug, T., Matzavinos, A., and Kuret, J. (2008) *J. Biol. Chem.* **283,** 13806–13816
39. Necula, M., and Kuret, J. (2004) *Anal. Biochem.* **329,** 238–246
40. Jeganathan, S., Hascher, A., Chinnathambi, S., Biernat, J., Mandelkow, E. M., and Mandelkow, E. (2008) *J. Biol. Chem.* **283,** 32066–32076
41. Liu, F., Li, B., Tung, E. J., Grundke-Iqbal, I., Iqbal, K., and Gong, C. X. (2007) *Eur. J. Neurosci.* **26,** 3429–3436
42. Sato, S., Tatebayashi, Y., Akagi, T., Chui, D. H., Murayama, M., Miyasaka, T., Planel, E., Tanemura, K., Sun, X., Hashikawa, T., Yoshioka, K., Ishiguro, K., and Takashima, A. (2002) *J. Biol. Chem.* **277,** 42060–42065
43. Rankin, C. A., Sun, Q., and Gamblin, T. C. (2007) *Mol. Neurodegener.* **2,** 12
44. Noble, W., Planel, E., Zehr, C., Olm, V., Meyerson, J., Suleman, F., Gaynor, K., Wang, L., LaFrancois, J., Feinstein, B., Burns, M., Krishnamurthy, P., Wen, Y., Bhat, R., Lewis, J., Dickson, D., and Duff, K. (2005) *Proc. Natl. Acad. Sci. U.S.A.* **102,** 6990–6995
45. Perez, M., Hernandez, F., Lim, F., Diaz-Nido, J., and Avila, J. (2003) *J. Alzheimers Dis.* **5,** 301–308
46. Bhat, R., Xue, Y., Berg, S., Hellberg, S., Ormo, M., Nilsson, Y., Radesater, A. C., Jerning, E., Markgren, P. O., Borgegard, T., Nylof, M., Gimenez-Cassina, A., Hernandez, F., Lucas, J. J., Diaz-Nido, J., and Avila, J. (2003) *J. Biol. Chem.* **278,** 45937–45945
47. Wischik, C. M., Edwards, P. C., Lai, R. Y., Roth, M., and Harrington, C. R. (1996) *Proc. Natl. Acad. Sci. U.S.A.* **93,** 11213–11218
48. Heiser, V., Scherzinger, E., Boeddrich, A., Nordhoff, E., Lurz, R., Schugardt, N., Lehrach, H., and Wanker, E. E. (2000) *Proc. Natl. Acad. Sci. U.S.A.* **97,** 6739–6744
49. Smith, D. L., Portier, R., Woodman, B., Hockly, E., Mahal, A., Klunk, W. E., Li, X. J., Wanker, E., Murray, K. D., and Bates, G. P. (2001) *Neurobiol. Dis.* **8,** 1017–1026
50. Tseng, H. Y., Wu, S. H., Huang, W. H., Wang, S. F., Yang, Y. N., Mahindroo, N., Hsu, T., Jiaang, W. T., and Lee, S. J. (2005) *Bioorg. Med. Chem. Lett.* **15,** 2027–2032
51. Tsai, C. C., Lin, M. T., Yang, C. C., Liao, J. F., and Lee, J. J. (2006) *Shock* **26,** 601–607
52. Licha, K., Riefke, B., Ntziachristos, V., Becker, A., Chance, B., and Semmler, W. (2000) *Photochem. Photobiol.* **72,** 392–398
53. Volkova, K. D., Kovalska, V. B., Balanda, A. O., Vermeij, R. J., Subramaniam, V., Slominskii, Y. L., and Yarmoluk, S. M. (2007) *J. Biochem. Biophys. Methods* **70,** 727–733